

## An Updated Plasma Scenario for the Spherical Tokamak for Energy Production

H. Meyer for the STEP Plasma Development Team and Contributors  
UK Fusion Energy Ltd., Culham Campus, Abingdon, Oxon, OX3 7RZ, UK  
E-mail (speaker): hendrik.meyer@ukifs.uk

The UK's Spherical Tokamak for Energy Production (STEP) programme, aiming to provide a prototype fusion power plant (SPP) based on the spherical tokamak concept targeting 2040 [1], has now moved from the conceptional to the preliminary design phase. Key objectives of the SPP, which will drive the creation of a UK fusion economy, are to deliver net electric power  $P_{\text{net}} > 100$  MWe and demonstrate tritium self-sufficiency. Choosing a fully non-inductive flat top operating point without inboard breeding drives the design to low aspect ratio  $A \sim 1.8$ , high elongation  $\kappa \sim 3$  and high normalised plasma pressure  $\beta_N \sim 4$  [2] as fusion power scales as  $P_{\text{fus}} \propto (\beta_N B_t)^4 \kappa^5 (R_{\text{geo}}/A)^3$  at high bootstrap current fraction  $f_{\text{BS}} = I_{\text{BS}}/I_p \sim 0.8 - 0.9$ . The high  $f_{\text{BS}}$  reduces the demand on the auxiliary microwave based heating and current drive system on STEP. In addition to the usual electromagnetic electron cyclotron wave current drive (ECCD), the use of electrostatic electron Bernstein waves current drive (EBCD) combined with ECCD is considered [3]. EBCD provides normalised current drive efficiency that is up to 3 times higher than ECCD and potentially creates opportunities to access scenarios at commercial power plant-relevant fusion gain,  $Q = P_{\text{fus}}/P_{\text{aux}} \sim 30$ . The ECCD scenario operates at  $Q \sim 11$ . Since publishing the original design base (SPP-1) ( $R_{\text{geo},1} = 3.6$  m,  $B_{t,1} = 3.2$  T,  $I_{p,1} \leq 23$  MA,  $1.5$  GW  $\leq P_{\text{fus}} \leq 1.8$  GW in 2025) [1], to reduce the risk to the centre column, the design has moved to a larger baseline (SPP-2) with  $R_{\text{geo},2} = 4.3$  m,  $B_{t,1} = 3$  T but with the same fusion power range and aspect ratio, leading to a similar  $I_p$ . Plasma solutions for the larger design have proven to be more challenging in some areas, while making it easier to find an exhaust solution. To handle the heat load in the divertor at this high fusion power a core radiation fraction  $f_{\text{rad}} = P_{\text{rad}}/P_{\text{heat}} \sim 0.7$  is adopted.

Recent efforts to explore solutions with lower recirculating power have led to a change of assumptions. On the one hand, with dedicated R&D it seems reasonable to assume an increase of the wall plug efficiency for the HCD system from  $\eta_{\text{HCD}} = 0.4$  to  $\eta_{\text{HCD}} = 0.6$ , which for a  $Q \sim 10$  device has a significant impact on the  $P_{\text{fus}}$  required to achieve  $P_{\text{net}} \gtrsim 100$  MW. On the other hand, reducing the core radiation fraction to 0.5 and operating slightly above the empirical Greenwald density limit ( $f_{\text{GW}} = n/n_{\text{GW}} \leq 1.4$ :  $n_{\text{GW}} = I_p(\text{MA})/(\pi a^2)[10^{20} \text{m}^{-3}]$ ) allows for a more efficient core plasma solution at lower  $P_{\text{fus}}$  and  $I_p$ . Operating with  $f_{\text{GW}} > 1$  has been experimentally demonstrated on devices like ASDEX Upgrade, DIII-D and MAST using pellet fuelling. Overall, flat-top operating points (FTOP) with  $P_{\text{fus}} \sim 1$  GW and  $I_p \leq 18$  MA seem to be feasible without taking advantage of the opportunities given by EBCD. The lower plasma current reduces the disruption challenge notably, but the lower radiation fraction puts more stringent requirements on the exhaust solution and is likely to be limited by the tolerable Ar concentration at the last closed flux surface (LCFS). In addition, independent core radiation control using Xe may not be possible, increasing the plasma control challenge.

The new assumptions have also been used to reduce the device size again. This is not only more cost effective but also makes quench protection of the toroidal field system less challenging by lowering the magnetic energy in the system. The experience of SPP-1 and SPP-2 shows that a reduction of the TF coil volume and therefore of the magnetic energy in the TF system is only possible by increasing the aspect ratio. Explorations of the design space with the 1.5 D integrated transport solver JETTO in assumption integration mode and the system code PROCESS using the learning from the previous design points and freedom in the range of  $P_{\text{fus}}$  have led to the identification of a new net power scenario with  $A = 2$ ,  $R_{\text{geo}} = 4$  m,  $B_t(R_{\text{geo}}) = 3.2$  T,  $I_p \sim 16$  MA,  $f_{\text{rad}} = 0.5$ ,  $f_{\text{GW}} \sim 1.3$ ,  $\kappa = 2.8$ ,  $\delta \sim 0.65$ ,  $P_{\text{fus}} \sim 1$  GW and  $P_{\text{ECCD}} \sim 120$  MW but requiring a slightly more aggressive transport assumption of  $\langle H_{98(y,2)} \rangle = (H_{98(y,2)} + H_{98(y,2)}^*)/2 = 1.41$  using the ITER physics basis confinement scaling law [4], where  $H$  and  $H^*$  denote the confinement enhancement factor with and without the core radiation taken into account respectively. Using the Petty et.al. scaling law for confinement [5], which takes the results of dimensionless scaling experiments into account, this equates to  $\langle H_{\text{Petty08}} \rangle \sim 1$ . This should only be taken as indicative, since both scaling laws were obtained using data in a different turbulence regime to STEP. One of the reasons for the more challenging confinement assumption is that a

refinement of the bootstrap current,  $I_{BS}$ , calculation in JETTO led to a 15% reduction due to an overestimation of the trapped particle fraction for the extreme shaping of STEP. Detailed comparison of  $I_{BS}$  models with the NEO code show that  $I_{BS}$  is now accurately predicted in JETTO. With the reduced  $I_{BS}$  the SPP-2 design point has  $\beta_N \sim 4.8$  and  $\langle H_{98(Y,2)} \rangle \sim 1.6$ , which is challenging for resistive wall mode (RWM) control and core transport. For the  $A = 2, R = 4 m$  both  $\beta_N \sim 4.2$  and  $\langle H_{98(Y,2)} \rangle \sim 1.4$  are less challenging, but the lower pedestal performance at the lower plasma current leads to a pressure peaking that is still marginal for RWM control with  $C_\beta = (\beta_N - \beta_N^{iw}) / (\beta_N^{nw} - \beta_N^{iw}) \sim 0.5$  ( $\beta_N^{nw, iw}$  the no-wall and ideal wall  $\beta$  limit respectively). The compatibility of the  $A = 2, R = 4 m$  FTOP with respect to divertor performance and magnet requirements has been tested using an initial poloidal field coil set.

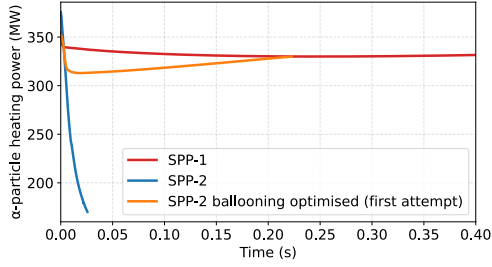


Figure 1:  $\alpha$ -particle heating power,  $P_\alpha$ , from a flux driven core transport calculations with (T3D-KBM) suggesting that a high-performance core plasma state could exist.

The physics basis for STEP has matured considerably, reducing uncertainties in plasma core performance, divertor performance, control and operations without type-I ELMs. The onset of high core transport fluxes in high  $\beta$  regimes with low torque input due to the dominant hybrid kinetic ballooning mode (hKBM) turbulence is now understood. The competition between the Reynolds and Maxwell stresses with respect to zonal flow generation leading to these high fluxes is governed by a threshold  $q^2 \beta_e = f(\hat{s}, \gamma_E)$  ( $\hat{s}$ : magnetic shear,  $\gamma_E$ :  $E \times B$  flow shear). This has been used to optimise the flat-top solution in SPP-2. Figure 1 shows modelling of the  $\alpha$ -heating power using a quasi-linear reduced core transport model capturing the hKBM transport [6] in the T3D framework (T3D-KBM). This model does not evolve the equilibrium self consistently nor does it include the effects of impurities and  $\alpha$ -particles. Starting with the initial FTOP profiles from the assumption integration simulations with JETTO, the T3D modelling for SPP-1 predicts a high performance state where the turbulent fluxes are consistent with the input power. Applying a similar approach to an initial SPP-2 point (blue) does not lead to a consistent solution but rather collapses into a low performance state. However, optimising the pressure and q-profile of the SPP-2 FTOP (orange) with respect to the onset of the high flux states leads to the recovery of a consistent high performance state. Whilst this gives some confidence in the existence of a plasma solution compatible with net electricity production, access to it from a low  $\beta$  state is still to be resolved. It should also be noted that the modelling is very sensitive to the choice of initial conditions such as flow shear or the radiation fraction. Here, the pedestal pressure is a fixed boundary condition.

The stability of Alfvénic modes has been assessed using the HALO code for toroidicity induced Alfvén eigenmodes (TAE) and ellipticity induced AEs (EAE) in the SPP-2 flat-top. As expected in a burning plasma device, the drive of these modes by  $\alpha$ -particles is strong. Nevertheless, neither TAEs nor EAEs should be unstable in STEP as at high  $\beta$  the Alfvén velocity is closer to the ion thermal velocity than in conventional aspect ratio tokamaks, leading to bulk ion Landau damping that is stronger than the drive.

Although most scenario exploration is performed using JETTO or RAPTOR with  $\beta_N$  feedback used to achieve the required  $P_{fus}$ , codes that include an ST-optimised version of TGLF and a newly developed quasilinear model for hKBM transport provide flux-driven predictive capabilities. Machine learning has been used to provide surrogates for faster scenario evaluation. The performance of TGLFNNv1, a low-density ST-optimised

The physics basis for STEP has matured considerably, reducing uncertainties in plasma core performance, divertor performance, control and operations without type-I ELMs. The onset of high core transport fluxes in high  $\beta$  regimes with low torque input due to the dominant hybrid kinetic ballooning mode (hKBM) turbulence is now understood. The competition between the Reynolds and Maxwell stresses with respect to zonal flow generation leading to these high fluxes is governed by a threshold  $q^2 \beta_e = f(\hat{s}, \gamma_E)$  ( $\hat{s}$ : magnetic shear,  $\gamma_E$ :  $E \times B$  flow shear). This has been used to optimise the flat-top solution in SPP-2. Figure 1 shows modelling of the  $\alpha$ -heating power using a quasi-linear reduced core transport model capturing the hKBM transport [6] in the T3D framework (T3D-KBM). This model does not evolve the equilibrium self consistently nor does it include the effects of impurities and  $\alpha$ -particles. Starting with the initial FTOP profiles from the assumption integration simulations with JETTO, the T3D modelling for SPP-1 predicts a high performance state where the turbulent fluxes are consistent with the input power. Applying a similar approach to an initial SPP-2 point (blue) does not lead to a consistent solution but rather collapses into a low performance state. However, optimising the pressure and q-profile of the SPP-2 FTOP (orange) with respect to the onset of the high flux states leads to the recovery of a consistent high performance state. Whilst this gives some confidence in the existence of a plasma solution compatible with net electricity production, access to it from a low  $\beta$  state is still to be resolved. It should also be noted that the modelling is very sensitive to the choice of initial conditions such as flow shear or the radiation fraction. Here, the pedestal pressure is a fixed boundary condition.

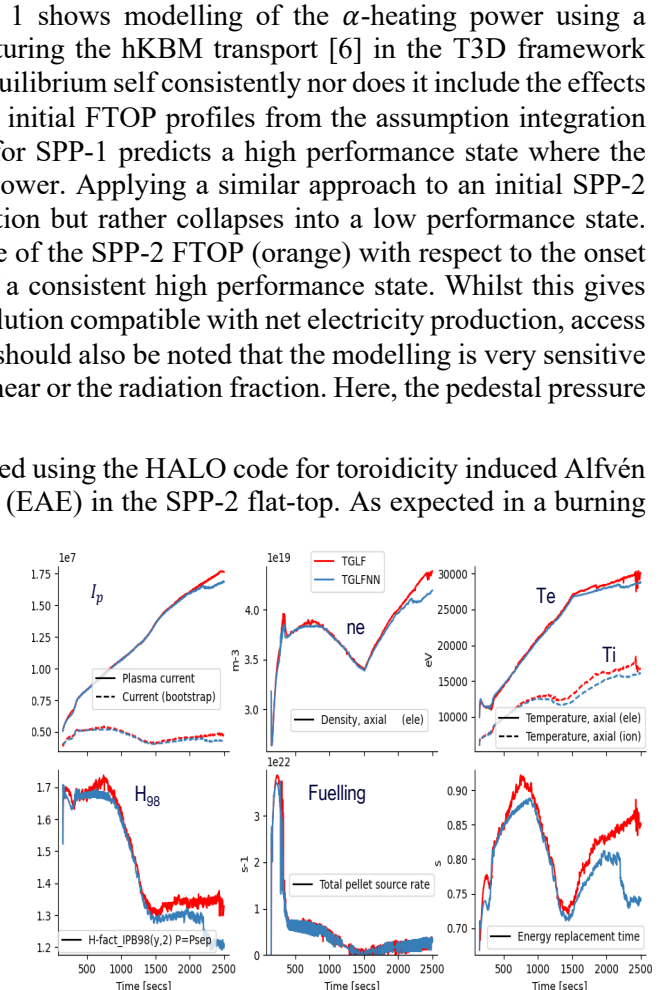


Figure 2: Comparison typical time traces of predictive JETTO simulations for the low-density non-inductive ramp-up phase to high current with the ST optimized TGLF (red) model and the neural network surrogate TGLFNNv1 (blue).

surrogate for TGLF, is shown in Figure 2, comparing typical time traces for simulations of a low-density fully non-inductive ramp-up to high plasma current. An important phase for the whole plant design is the onset of the plasma burn as the plasma density is increased. Initially it was envisaged to do this quickly,  $\mathcal{O}(10s)$ , to optimise the trade-off between auxiliary-driven and bootstrap current. Following control and predictive modelling, the time for the access to fusion burn has now been slowed to  $\Delta t_{burn} \gtrsim 300s$  to mitigate implications on the wider plant.

An optimised divertor design has been developed to provide good detachment access and efficient He exhaust at the same time. This features a novel extended dome design as well as an optimised pump duct position. On STEP direct pumping of the inner divertor legs is difficult to realise and the He must therefore be exhausted using a pump in the outer divertor. He recycled in the inner divertor can enter the core through the X-point region, leading to intolerably high He concentrations in the core. This can be avoided by optimising the inner under-dome passage opening with respect to the inner strike point. A vertical outer target configuration with pumping from the private flux region (PFR) close to the strike point would give the best results in terms of He exhaust but is the worst solution with respect to achieving detachment, whilst a horizontal target with pumping from the scrape-off-layer (SOL) away from the strike point optimises the detachment onset. Placing the pump duct opening approximately horizontally aligned with the low field side dome outflow and co-aligning the detachment front with both provides sufficient He pumping whilst retaining good detachment access.

The first coupled core edge simulations using JETTO and EDGE2D (COCONUT) are being used to understand the impact of He and Ar on scenario performance. These computationally expensive, complex simulations are still using the SPP-1 design with a non-optimised dome and are performed for He and Ar as impurities separately without drifts enabled in EDGE2D. Here NCLASS is used for core impurity transport. For He, advanced simulation control would be needed to get stable solutions with a fixed Bohm-Gyro-Bohm transport assumption. In the absence of this the initial calculations to determine suitable He pumping speeds  $S_{He}$  are done in two steps [7]. First, COCONUT simulations with  $\beta_N$  (fusion power) control are used to determine the relation between the  $S_{He}$  and the He density at the separatrix  $n_{He}^{sep}$ . Then scans of the pedestal pressure and energy confinement time are used to determine the fusion performance. These calculations show that  $S_{He} \approx (50 \pm 20) m^3/s$  would be likely to provide adequate He exhaust if there is no turbulent inward particle pinch, as indicated by the hKBM modelling. COCONUT modelling for SPP-1 has been performed to determine the tolerable Ar seeding rate. As mentioned above, the radiated power due to Ar entering the core can be substantial. In addition to the COCONUT modelling, the fast FACIT code as well as the most complete JETTO+NEO models have been used to determine neoclassical Ar transport in the pedestal with FACIT and NEO showing good agreement with respect to the Ar screening. The 1D SOL code DART is used to relate detachment onset to the Ar concentration at the separatrix and the neutral pressure in the divertor. This modelling indicates that at  $f_{rad} \sim 0.5$  a tolerable Ar concentration can be achieved but at higher divertor neutral pressures of  $15 Pa \leq p_{div} \leq 20 Pa$ . However, SOLPS-ITER simulations for SPP-1 with both He and Ar as impurities including drifts indicate that simulations without drifts may underestimate the Ar content in the core. The simulations show a 50% higher Ar content originating from the low field side main chamber SOL. This was due to an increased escape of Ar from the lower outer divertor, fed by increased leakage of neutral Ar from the lower inner divertor. With drifts active, Ar accumulation rises by an order of magnitude in the lower inner divertor due to strongly-enhanced parallel flow of Ar in the high field side SOL leading in these simulations to a different detachment state in the inner and outer divertor legs, which can likely be mitigated by asymmetric Ar seeding in the four divertor legs.

Vertical control is critical, due to the need to keep the plasma in an exact double null (DN) configuration where the parallel heat flux to the inner divertor is minimised [8]. Exact DN is also important to enable good access to H-mode [9]. The SOL decay length is expected to be only  $\lambda_{SOL} \sim (1 - 2) mm$  and the accuracy required of the vertical control is thus very high. A novel DN control scheme that allows independent control of the vertical position and the difference in poloidal flux between the X-points has been developed. Initial tests on TCV [10] show that accurate DN balancing and constant power distribution between all four divertor legs is maintained during substantial pre-programmed shifts in vertical position. Whilst the control on similar time scales has not yet been demonstrated, modelling of this for STEP is encouraging and the engineering implications for the STEP design are being accessed.

A new kinetic controller with an adaptive observer (AO) and adaptive model predictive control (AMPC) enables the assessment of burn control in the context of measurement and model uncertainties. Here, the RAPTOR code is used as a plasma model. Multi objective control is tested using unrealistically fast steps in fusion power. The AO uses a nonlinear RAPTOR process model to predict the state and to generate a linearised model that is fed into the AMPC to calculate an optimised trajectory for the next 50 s. Data from a sparse stochastic measurement set are compared to virtual measurements that are mapped from the state prediction. The differences between the measured and predicted quantities are used to update the physics model as well as parameter estimates. The new updated linearised model is then fed into the AMPC for a new trajectory optimisation. Disturbances on the physics model in RAPTOR are used to mimic potential differences between the plasma model and the physical plasma as the latter is not yet known. Even without measurement errors or disturbances, it is not possible to tightly control all quantities of interest such as the q-profile and internal inductance. However, control within tolerable bands that don't violate hard constraints is possible. Satisfactory control within the constraints is still maintained after adding  $1\sigma \leq 10\%$  errors and some disturbances in heat diffusivity, resistivity,  $\alpha$ -power and bootstrap current density, provided that sufficient auxiliary heating power is installed. This framework is now being used to develop requirements for the plasma diagnostic set and the actuators.

Disruptions are a major threat to any tokamak-based power plant concept. The reduction in plasma current and stored plasma energy achieved by the new assumption set reduces the engineering challenge posed by disruptions. The highest risk during a disruption is the generation of a runaway electron (RE) beam. Early modelling in SPP-1 suggested that shattered pellet injection (SPI) alone might not be enough to mitigate the RE beam [11]. Therefore, an RE mitigation coil (REMC) has been incorporated into the design to enable dissipation of the RE current in combination with SPI. Deconfinement of the RE beam for several mock RE equilibria with a given REMC design has been modelled for several values of the REMC current using the orbit following code LOCUST. The calculated currents are used in the engineering design to assess the forces on the coil, which will set the limit for this method of RE mitigation. From this modelling it seems feasible that  $> 75\%$  of the REs can be deconfined in less than 0.1 ms.

Using MAST-U and other tokamaks, experimental validation of the codes and assumptions has progressed. Experiments on EBW heating on TCV have confirmed the predictions by the CRAYON code – a key design tool for STEP – showing record coupling efficiencies  $\geq 80\%$ . Good agreement between CRAYON simulations and EBW emission on MAST-U gives further confidence in the modelling. The achievement of ELM suppression on MAST-U for the first time in an ST is another example of how STEP plasma risks are being burned down.

A manageable R&D programme to develop key diagnostic systems for STEP is being established. Considerable progress has been made in STEP scenario modelling capability but still many challenges remain. The burning plasma solution is driving physics development at the forefront of fusion research.

*This work has been funded by STEP, a major technology and infrastructure programme led by UK Fusion Energy Ltd (UKFE), which aims to deliver the UK's prototype fusion powerplant and a path to the commercial viability of fusion.*

- [1] C. Waldon, S. I. Muldrew, J. Keep, R. Verhoeven, T. Thompson, and M. Kisebey-Ascott, *Philosophical Transactions of the Royal Society A: Mathematical, Physical and Engineering Sciences* **382**, 20230414 (2024).
- [2] H. Meyer and on behalf of the STEP Plasma Team, *Philosophical Transactions of the Royal Society A: Mathematical, Physical and Engineering Sciences* **382**, 20230406 (2024).
- [3] S. Freethy, L. Figini, S. Craig, M. Henderson, R. Sharma, T. Wilson, and S. t. the, *Nuclear Fusion* **64**, 126035 (2024).
- [4] ITER Physics Expert Group on Confinement and Transport, ITER Physics Expert Group on Confinement Modelling Database, and ITER Physics Basis Editors, *Nuclear Fusion* **39**, 2175 (1999).
- [5] C. C. Petty, *Physics of Plasmas* **15**, 80501 (2008).
- [6] M. Giacomini *et al.*, *Journal of Plasma Physics* **91**, E16, E16 (2025).
- [7] E. Tholerus, in *30th IAEA Fusion Energy Conference* Chengdu, China, (2025).
- [8] R. T. Osawa, D. Moulton, S. L. Newton, S. S. Henderson, B. Lipschultz, and A. Hudoba, *Nuclear Fusion* **63**, 076032 (2023).
- [9] H. Meyer *et al.*, *Nuclear Fusion* **46**, 64 (2006).
- [10] M. Lafferty, O. Bardsley, C. Heiss, and A. Mele, *IEEE Transactions on Plasma Science*, 1 (2026).
- [11] A. Fil, L. Henden, S. Newton, M. Hoppe, and O. Vallhagen, *Nuclear Fusion* **64**, 106049 (2024)